

Paul L. Smith*, Fred J. Kopp, and Harold D. Orville
South Dakota School of Mines & Technology
Rapid City, South Dakota

1. Introduction

Atmospheric water budgets are commonly derived from integration of expressions such as

$$\frac{\partial W}{\partial t} + \frac{1}{A} \oint_S \vec{Q} \cdot \vec{n} ds = E - P \quad (1)$$

over some area A for the appropriate time interval. Here W represents the precipitable water stored in the atmosphere; \vec{Q} is the moisture flux vector, with \vec{n} being a unit normal vector directed outward from the perimeter of the area A . The surface integral around the vertical boundary S of the area represents the moisture divergence. For storm-scale calculations both W and \vec{Q} should include condensate, but for more extensive domains, only the vapor component may be significant. The quantities E and P represent evapotranspiration and precipitation rates, respectively. Each term in (1) has units of m/s, or more conveniently mm/day. For comparison, 1 mm of water covering an area of 1 km² is 10³ m³ (1 kiloton) of water, or about 0.81 acre-ft.

For many situations the change of W with time may be negligible and the first term in (1) can be neglected. Also, reasonable estimates of P are usually available. The greatest challenges in applying (1) are in determining the divergence and evapotranspiration terms. The evapotranspiration problem is ubiquitous, and critical issues of spatial and temporal resolution commonly arise in establishing the divergence term. In complex terrain, further difficulties crop up in using typical data on atmospheric profiles of water vapor and wind to estimate the divergence term. Those difficulties are the subject of this paper; considerations related to topographic variations both along and normal to the flow direction are treated.

2. Background

Moisture divergence calculations commonly involve terms of the form $\frac{\partial Q_x}{\partial x}$ or a finite difference approximation thereto. In sloping terrain, things become a bit more complicated. Schaefer (1973) and Bluestein and Crawford (1997) treated the problem by

*Corresponding author address: Paul L. Smith, Institute of Atmospheric Sciences, South Dakota School of Mines & Technology, 501 E. St. Joseph, Rapid City, SD 57701-3995.

considering the vertical gradient of the quantity of interest. For the wind velocity, for example, they took

$$\left. \frac{\partial u}{\partial x} \right|_h = \frac{\partial u}{\partial x} + \frac{\partial h}{\partial x} \cdot \frac{\partial u}{\partial z} \quad (2)$$

where h represents the terrain height. For application to (1), it would have to apply as well for height h above the terrain. The simple example in Figure 1 shows that this cannot be correct for complex terrain, though the approximation may be adequate for the gentle terrain slopes (of order 1 m/km) in their situations. The idealized wind profiles in Figure 1 have no shear, but even with

$$\left. \frac{\partial u}{\partial x} \right|_h = 0 \quad \text{and} \quad \frac{\partial u}{\partial z} = 0 \quad (3)$$

there is clearly divergence in the domain represented.

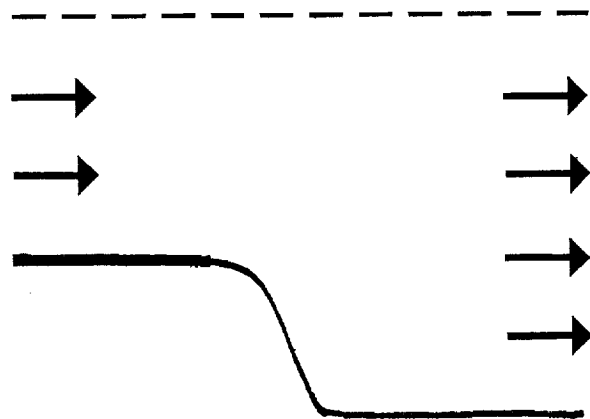


Fig. 1: Schematic of an idealized situation with a uniform wind and varying terrain elevation.

The divergence calculation could in principle be handled by direct calculation of the fluxes across the boundaries of the area, as suggested by the surface integral in (1). However, the topography normal to the flow direction introduces another set of complications. Consider the situation in Figure 2, where neighboring atmospheric sounding sites are located at two different altitudes, with a monotonic variation in the intervening terrain. Suppose further that the moisture flow is normal to the figure. Linear interpolation, or more complicated standard methods, can be used to estimate the values of wind speed and vapor concentration in the free atmosphere at Level B. At Level A, however, the appropriate procedure is less clear; some method of determining the conditions at the point where Level A intersects the surface would be needed to permit

similar interpolation, and simple linear interpolation may not even be appropriate here. For estimating the surface wind conditions, terrain elevation seems to be the most critical factor (Weber 1990; Palomino and Martin 1995). The flow component normal to the diagram may also be a factor, since barrier-normal and barrier-parallel flows differ in character. Model simulations may provide helpful information (e.g. Pielke 1985). Such things as slope/valley winds and wave effects can be important under some circumstances. Estimating the wind values for Level A is only part of the problem, and methods for interpolating the humidity values at the surface, or aloft, have been much less studied.

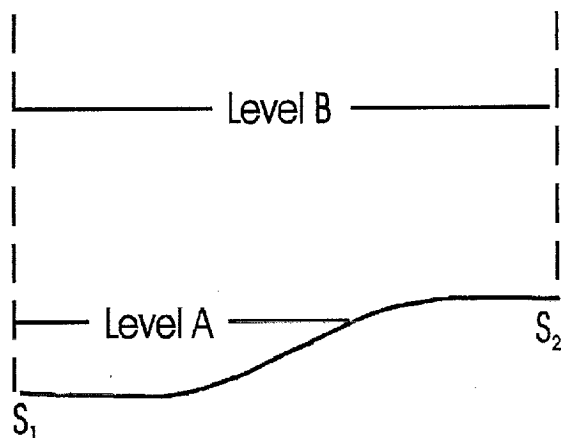


Fig. 2: Schematic of a situation with soundings at two sites (S_1 , S_2) at different elevations.

3. An Analytical Approach

For situations similar to Figure 2, an analytical approach may be useful. Consider some function F , say the eastward component of the atmospheric moisture flux, that varies with position in space. If observations are available from four sounding sites enclosing the area of interest, a Taylor expansion of the function about one of the sites at x_0, y_0, z_0 gives

$$F(x, y, z) = F(x_0, y_0, z_0) + (x - x_0) \frac{\partial F}{\partial x} + (y - y_0) \frac{\partial F}{\partial y} + (z - z_0) \frac{\partial F}{\partial z} \quad (4)$$

Taking the soundings to represent layers (not necessarily horizontal, or even planar), at varying heights above the ground, the four observations for each layer provide three independent equations. Those can be solved for the gradients in that layer, which in turn permit calculations of F for positions in that layer. The important calculations for budget estimates are along the (vertical) walls of the area encompassed by the four sounding sites.

Upper Missouri River Basin Pilot Project data from the 1800 UTC soundings on 22 April 1999 in the Black Hills region of South Dakota and Wyoming provide example data. Figure 3 illustrates the project area, with rawinsonde sites at three corners and a microwave radiometer/wind profiler installation at the southern site. For convenience, the example calculations consider only a rectangle with east-west and north-south borders, with a sounding site near the center of each of those sides. Later calculations will treat the baseball-diamond-shaped interior area.

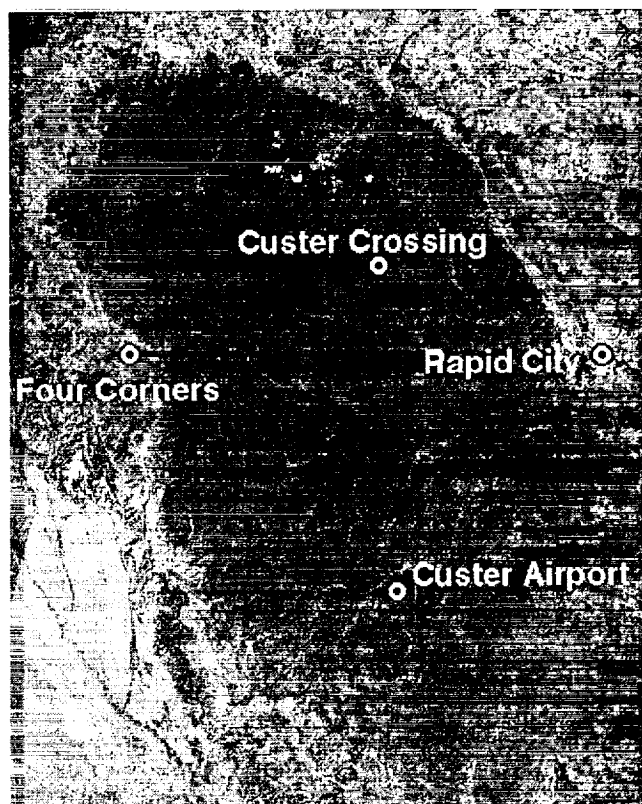


Fig. 3: Map of the Upper Missouri River Basin Pilot Project area, indicating the four sounding sites in the Black Hills of South Dakota and Wyoming. Map dimensions 100 x 30 km.

Figures 4 and 5 show the horizontal and vertical gradients, respectively, of the two flux components (eastward, northward). To determine these gradients, each sounding between the surface and 6 km MSL was interpolated to 50 equally-spaced layers; the layer altitudes varied among the soundings due to different surface elevations at the sites. Eastward and northward flux components were computed for each layer in each sounding. Then (4) was solved for the three gradients of each component in each layer, with the results indicated in the figures.

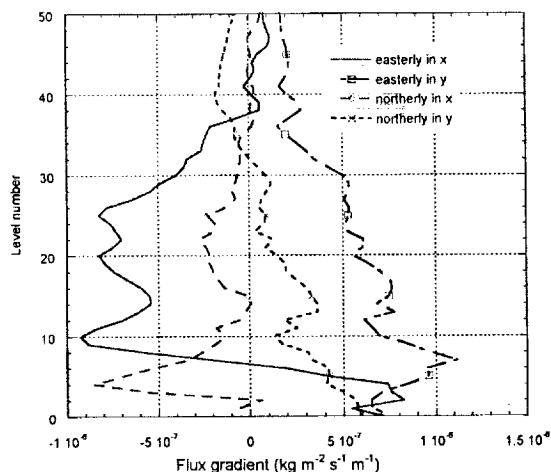


Fig. 4: Plot of the horizontal gradients in the eastward or northward components of the moisture flux for the 50 levels, determined by solving (4) using the four soundings from 1800 UTC 22 April 1999.

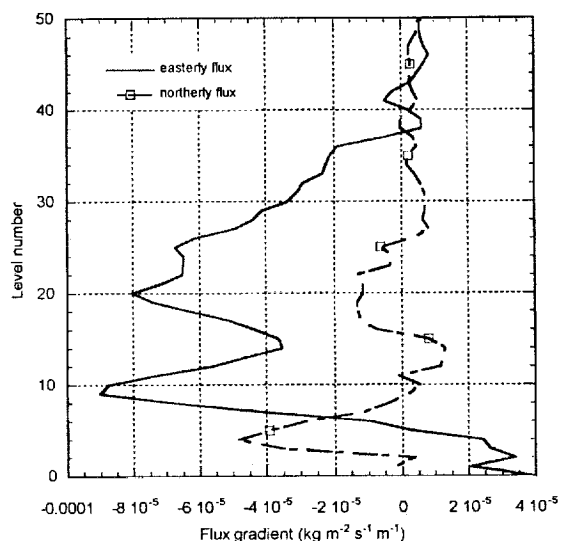


Fig. 5: As Fig. 4, showing the vertical gradients in the eastward or northward flux components.

Next the gradients were used to determine the flux components along the boundaries of the rectangle for each layer. Figure 6 shows the profile of calculated fluxes through each layer in the four "walls" of the project area. The predominant wind flow in this situation was easterly upslope, and the northward fluxes at the northern and southern boundaries of the rectangular area are generally smaller than the westward flux through the other two sides.

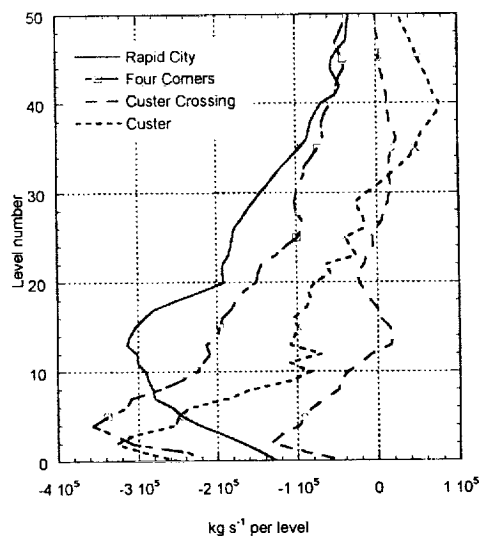


Fig. 6: Fluxes through the four walls for each of the 50 layers. Values are eastward for the eastern (Rapid City) and western (Four Corners) walls, and northward for the northern (Custer Crossing) and southern (Custer) walls.

Figure 7 shows flux values integrated from the surface upward. While the northward components are smaller, the net moisture divergence (represented by the difference between the two curves at the topmost level) exceeds the convergence represented by the difference between the curves for the two eastward components. These observations were taken during a significant precipitation episode in the Black Hills; unless the change in stored moisture (W) was significant, these results are indicative of the uncertainties in this procedure when applied to an area of order 4000 km².

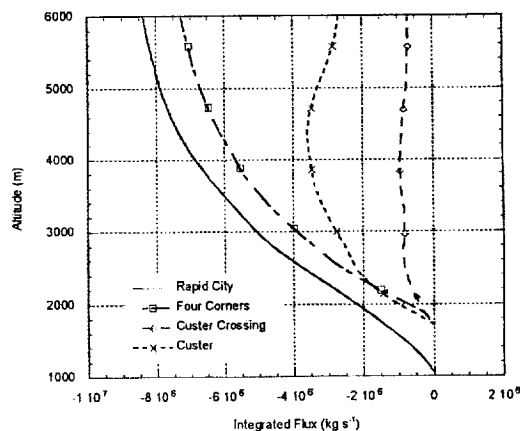


Fig. 7: Vertically integrated flux through each of the boundaries of the area, plotted as a function of MSL height. Difference between the eastward components at Rapid City and Four Corners at the 6 km level indicates (assuming negligible effects at higher altitudes) net moisture convergence in the eastward flow. Similarly, difference between the northward components at Custer and Custer Crossing indicates net divergence in the northward flow.

A similar calculation considering only the air mass flux through the four walls indicates no mass divergence in the eastward components (Fig. 8). However, the difference in the northward components suggests significant mass divergence. This is a further indication of appreciable uncertainty in the moisture divergence results. The problem may be related to different properties of the profiler/radiometer observations at the southern (Custer) site.

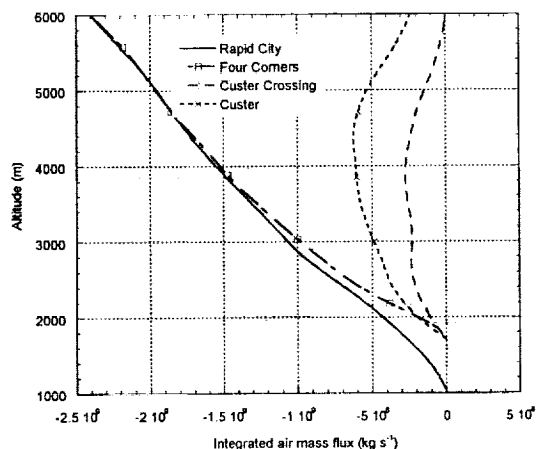


Fig. 8: Plot similar to Fig. 7, showing the air mass flux components computed in the same way. The eastward components at Rapid City and Four Corners agree closely, indicating no divergence. However, the substantial difference in the northward components indicates substantial mass divergence, indicating suggesting uncertainty in the results.

4. Complex Terrain

More complex terrain like that illustrated in Figure 9 will require a different approach. A key issue will be how to interpolate the observations along Level A; this basically requires projection of surface observations from Site 1 and/or Site 2. For the topography in Figure 9, the same approach as that for Figure 2, using relevant observations on either side of the intervening summit, may be appropriate. The role of the dimension perpendicular to the diagram must be considered, since the summit may separate air masses with different characteristics. For more complicated undulating peak and valley situations, the best procedure remains to be established. The complex variety of slope/valley winds, mountain-induced waves, and atmospheric stratifications somehow has to be taken into account.

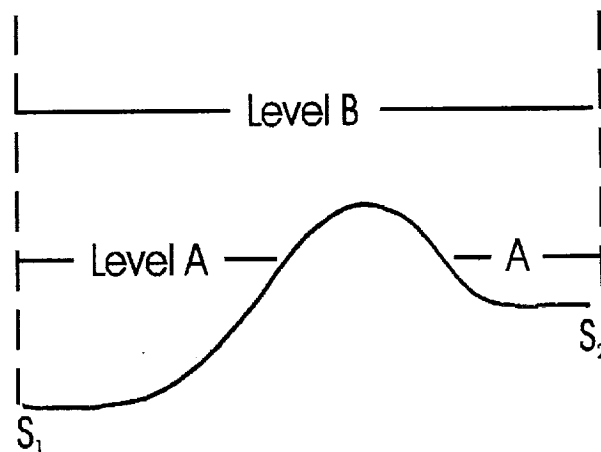


Fig. 9: Schematic illustration of the interpolation problem in mountainous terrain.

Acknowledgments. This work was conducted as part of the GCIP Upper Missouri River Basin Pilot Project, with support from NASA under Grant No. NAG8-1449.

References

- Bluestein, H.B. and T.M. Crawford, 1997: Dynamics of the near-dryline environment: Analysis of data from COPS-91. *Mon. Wea. Rev.*, **125**, 2161-2175.
- Palomino, I., and F. Martin, 1995: A simple method for spatial interpolation of the wind in complex terrain. *J. Appl. Met.*, **34**, 1678-1693.
- Pielke, R.A., 1985: The use of mesoscale numerical models to assess wind distribution and boundary layer structure in complex terrain. *Bound-Layer Meteor.*, **31**, 217-231.
- Schaefer, J.T., 1973: On the computation of the surface divergence field. *J. Appl. Meteor.*, **12**, 546-547.
- Weber, R., 1990: Interpolation of the wind field in a terrain following coordinate system over complex topography. *Atmos. Environ.*, **24**, 1971-1972.